

## Potential Structure Modified by Electron Cyclotron Resonance in a Plasma Flow along Magnetic Field Lines with Mirror Configuration

T. Kaneko, R. Hatakeyama, and N. Sato

*Department of Electronic Engineering, Tohoku University, Sendai 980-8579, Japan*

(Received 21 July 1997)

A plasma potential structure is modified by the electron cyclotron resonance (ECR) in a collisionless plasma flow along magnetic field lines with simple mirror configuration. In the presence of a single ECR point at the bottom of the magnetic well, there appears a potential dip (thermal barrier) around this point, being followed by a potential hump (plug potential) in the downstream side. The result in this simplified configuration gives a clear-cut physics to the formation of field-aligned plug potential with thermal barrier. [S0031-9007(98)05529-X]

PACS numbers: 52.58.Qv, 52.35.Nx, 52.50.Gj, 52.55.Jd

Plasma-potential formation in inhomogeneous magnetic fields is of great interest in conjunction with field-aligned particle acceleration, plasma confinement, and heat-transport reduction. In space plasmas, a field-aligned potential difference has been predicted to be generated by different pitch-angle anisotropies of electrons and ions along converging magnetic field lines [1], which was demonstrated in particle simulations [2] and in laboratory experiments [3]. The field-aligned potential difference due to double layers [4] has been proposed to play an important role in the aurora phenomena which have often been accompanied by intense wave emissions around the local electron cyclotron frequency [5]. In fusion-oriented plasmas, concepts of a plug potential with thermal barrier (plug/barrier potential) [6] and a thermal dike [7] have been proposed in order to realize the plasma confinement necessary for tandem-mirror devices and to reduce the heat transport in tokamak divertors, respectively. According to the original tandem-mirror scenario for the plug/barrier potential formation [8,9], a neutral beam injection (NBI) producing sloshing ions is necessary, in addition to the electron cyclotron resonances (ECR) at two positions with different magnetic fields in the end mirror cells. The recent experiment on the GAMMA 10 [10], however, indicates that this potential structure is formed without NBI in the presence of the two ECR points, although a physical mechanism of the potential formation has been unsolved. Actually, it is difficult to measure the overall field-aligned potential profiles in such a big fusion-oriented mirror device as the GAMMA 10 [8–11], and, thus, it has long been claimed to make an investigation under a simplified situation to clarify an essential mechanism of the potential formation due to the ECR.

In the presence of the ECR under a magnetic mirror field, the field-aligned magnetic force,  $-\mu \nabla B$ , acting on electrons increases, enhancing the electron trapping in the magnetic well, where  $\mu$  is the magnetic moment of electrons and  $\nabla B$  is the gradient of  $B$  in the direction parallel to magnetic field lines. Then, there appears an

electrostatic force acting on ions under the condition of charge neutrality. This mechanism provides a straightforward formation of a plug potential with thermal barrier in a plasma flowing along magnetic field lines with mirror configuration. Here we demonstrate this simple scenario for the plug/barrier formation. The physics of plug-potential formation is the same as that in the double-layer formation triggered by a small potential dip in current-carrying plasmas [12]. In our paper, in contrast to the double-layer formation, the scale length is much larger and the potential dip is produced by the mirror trapping of electrons in the plasma flow without electric current.

A plasma is produced by surface ionization of potassium atoms on a 5.0-cm-diam hot tungsten plate under an electron-rich condition and is confined by a magnetic field  $B$  of a few kG in a single-ended  $Q$  machine [13], as shown schematically in Fig. 1. Ions are accelerated by a potential drop of the electron sheath in front of the hot plate which is grounded electrically, together with a 20.8-cm-diam vacuum chamber. There is a grid (0.03-mm-diam wire, 50 mesh/in.) at a distance of 40 cm from the hot plate, which is biased negatively with respect to the hot plate. A step potential  $\phi_g$  is applied to the grid so as to increase the grid potential up to the plasma potential in order to inject a plasma flow along the magnetic field [3]. A small Langmuir probe is used to measure plasma parameters and their axial profiles. Under our

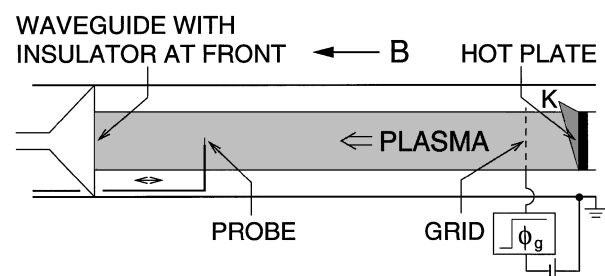


FIG. 1. Schematic of experimental setup. A plasma column, 5 cm in diameter and 310 cm long, is produced by surface ionization.

conditions, the plasma density  $n_{p0} \approx 1 \times 10^9 \text{ cm}^{-3}$ , the electron temperature  $T_{e0} \approx 0.2 \text{ eV}$ , the ion temperature  $T_{i0} \leq T_{e0}$ , and the ion flow energy  $E_{i0} \approx 10T_{e0}/e$ . A background gas pressure is  $4 \times 10^{-7} \text{ Torr}$ . The plasma is collisionless in the sense that collision mean free paths of electrons and ions are longer than the plasma length.

The experiment is carried out under a simple magnetic mirror configuration which is shown in the top figure in Fig. 2. The bottom of the magnetic well is located at the machine center ( $z = 0 \text{ cm}$ ). Mirror ratios  $R_d$  and  $R_u$  in the downstream ( $z < 0$ ) and upstream ( $z > 0$ ) regions are defined as ratios of  $B$  around  $z = -70 \text{ cm}$  and  $z = 100 \text{ cm}$ , respectively, to that at  $z = 0 \text{ cm}$ . A microwave with frequency  $\omega/2\pi = 6 \text{ GHz}$  and power  $P_\mu = 0-1 \text{ W}$  is launched into the plasma through a circular waveguide. The window of the waveguide is covered with an insulator which terminates the plasma column at  $z = -150 \text{ cm}$ . The microwave propagates toward the hot plate ( $z = 160 \text{ cm}$ ) in the region of  $\omega/\omega_{ce} < 1$  and the ECR takes place in the vicinity of  $\omega/\omega_{ce} = 1$  ( $\omega_{ce}/2\pi$ : electron cyclotron frequency) at  $z = 0 \text{ cm}$  (other situations are found in Ref. [14]). A

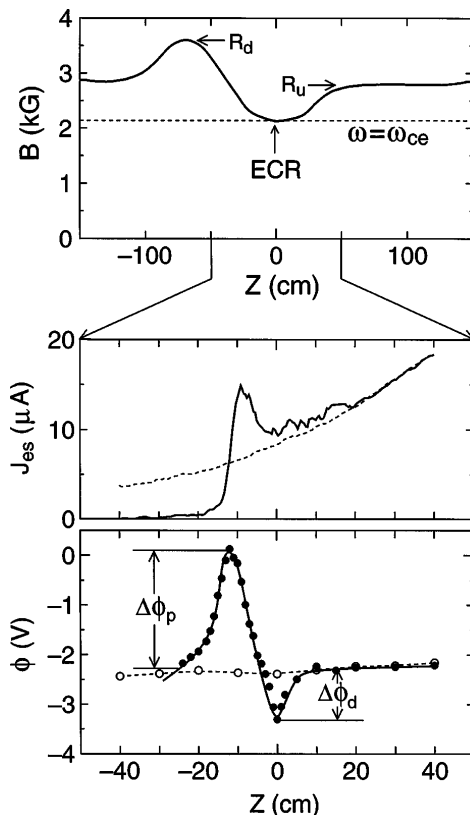


FIG. 2. A typical example of plasma flow plugging due to the ECR, together with magnetic field configuration. This shows profiles of  $J_{es}$  (electron saturation current of the probe) and  $\phi$  (plasma potential) at  $t = 0.6 \text{ ms}$  in the plasma flow injected at  $t = 0 \text{ ms}$  along the magnetic field with  $R_d = 1.68$  and  $R_u = 1.30$  for  $P_\mu = 0 \text{ W}$  (dotted lines) and  $0.5 \text{ W}$  (solid lines).

subscript 0 stands for the parameters in the case of  $P_\mu = 0 \text{ W}$ . Time resolved measurements are made by using a usual box-car sampling technique with time resolution of about  $1 \mu\text{s}$ , where probe-current pulses are averaged in a synchronous detection mode.

A typical example of the results in this experiment is presented in Fig. 2. Here, the plasma flow is injected at  $t = 0 \text{ ms}$  along the magnetic field with  $R_d = 1.68$  and  $R_u = 1.30$  for  $P_\mu = 0 \text{ W}$  (dotted lines) and  $0.5 \text{ W}$  (solid lines).  $J_{es}$  is the electron saturation current of the probe, which is proportional to the electron density multiplied by the electron thermal speed, and  $\phi$  is the plasma potential. The axial  $J_{es}$  and  $\phi$  profiles at the radial center, which are shown at  $t = 0.6 \text{ ms}$  in this figure, demonstrate clearly that the plasma flow is almost plugged by the potential structure produced by the ECR. This drastic plugging is also observed for the profiles of the plasma density obtained from  $J_{es}$ . The potential structure consists of a potential dip  $\Delta\phi_d (< 0)$  formed at  $z \approx 0 \text{ cm}$  and a subsequent potential hump  $\Delta\phi_p (> 0)$  along the plasma flow. Here,  $\Delta\phi_d$  and  $\Delta\phi_p$  are measured with respect to the potential in the upstream region, where  $\phi$  is almost constant spatially, being independent of  $P_\mu$ .

In Fig. 3, we present temporal evolutions of the  $J_{es}$  (solid lines) and  $\phi$  (solid lines with closed circles) profiles under the same conditions as in Fig. 2. Once the plasma front arrives at the ECR region, a clear increase of  $J_{es}$  in the ECR region and a drastic decrease of  $J_{es}$  in the downstream region appear together with a formation of the potential dip followed by the potential hump along

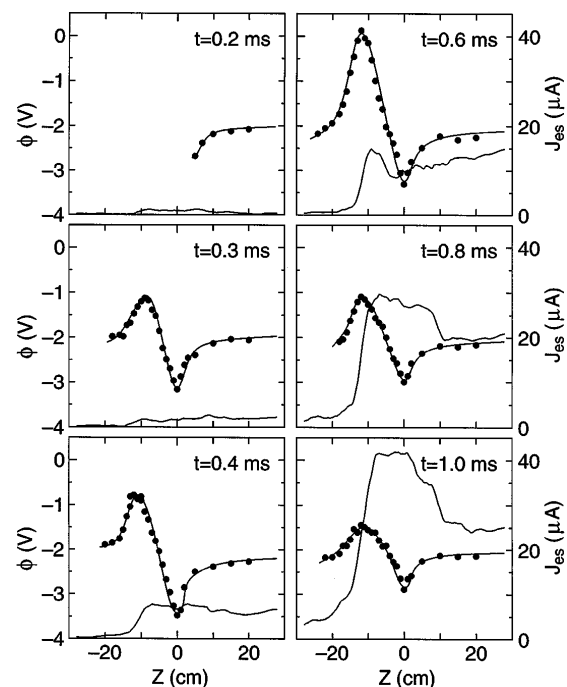


FIG. 3. Temporal evolutions of  $J_{es}$  (solid lines) and  $\phi$  (solid lines with closed circles) profiles after the plasma flow is injected at  $t = 0 \text{ ms}$  for  $P_\mu = 0.5 \text{ W}$ .

the plasma flow. After the potential dip ( $\approx -6T_{e0}/e$ ) is formed at  $t = 0.2\text{--}0.3$  ms,  $\Delta\phi_d$  is found to decrease temporally, gradually approaching a constant value ( $\approx -4T_{e0}/e$ ). On the other hand, the value of  $\Delta\phi_p$  has the maximum ( $\approx 10T_{e0}/e$ ) at  $t \approx 0.6$  ms which corresponds to the time necessary for the ion flow to arrive at the potential-hump position. At  $t > 0.6$  ms,  $\Delta\phi_p$  decreases temporally and approaches a constant value ( $\approx 3T_{e0}/e$ ) at  $t \approx 1.0$  ms. On the other hand,  $J_{es}$  at  $z \approx 0$  cm increases monotonously, approaching a constant value at  $t \approx 1.0$  ms. This decrease in  $\Delta\phi_p$  during the increase in  $J_{es}$  is ascribed to a change of the plasma in the upstream region after the ion reflection due to  $\Delta\phi_p$ . The ion reflection results in a reduction of the plasma flow speed, and then a smaller value of  $\Delta\phi_p$  can be sufficient for plugging the plasma flow. There appear density fluctuations of  $\tilde{n}_p/n_p = 0.1\text{--}0.2$ , especially at  $t \geq 0.6$  ms in our simple mirror geometry, which might also give rise to a decrease in the flow speed.

The potential structures at the time  $t = 0.6$  ms, when  $\Delta\phi_p$  has the maximum value, are presented with  $P_\mu$  as a parameter in Fig. 4, where  $R_d = 1.68$  and  $R_u = 1.30$ . For  $P_\mu = 0$  W, a small potential dip ( $\approx -T_{e0}/e$ ) is recognized in the magnetic well, agreeing with the result in Ref. [15]. In the case of  $P_\mu \neq 0$  W, however, even for  $P_\mu = 0.1$  W, there appears a clear modification of the potential structure. An increase in  $T_e$  is also observed at about  $z \approx 0$  cm for  $P_\mu \neq 0$  W.

Dependences of  $\Delta\phi_p$  and  $\Delta\phi_d$  on  $P_\mu$  at  $t = 0.6$  ms are presented for  $R_d = 1.68$  and  $R_u = 1.30$  in Fig. 5(a). With an increase in  $P_\mu$ , both  $\Delta\phi_p$  and  $-\Delta\phi_d$  increase,

gradually saturating for  $P_\mu > 0.5$  W. For  $P_\mu = 0.8$  W, we have  $e\Delta\phi_d \approx -7 T_{e0}$  and  $e\Delta\phi_p \approx 12 T_{e0}$ , which is of the order of the ion flow energy  $E_{i0}$ .  $T_e$  at  $z \approx 0$  cm increases in a quite similar way and yields a large difference of  $T_e$  between the upstream and downstream regions.  $T_e \approx 40T_{e0}$  and  $e\Delta\phi_p \approx 0.3T_e$  are found for  $P_\mu \approx 0.8$  W. This  $T_e$  increase, due to the ECR, is confirmed by a modified directional energy analyzer to be dominant in the direction perpendicular to the magnetic field, resulting in the anisotropic electron temperature. The perpendicular electron temperature is a key factor which links  $\Delta\phi_p$  with  $P_\mu$ , as found in the experiment on GAMMA 10 [16].

In Fig. 5(b),  $\Delta\phi_p$  and  $-\Delta\phi_d$  are plotted as a function of  $R_d$  at  $t = 0.6$  ms for  $P_\mu = 0.8$  W, where  $R_d \geq R_u > 1$  is kept. Both  $\Delta\phi_p$  and  $-\Delta\phi_d$  increase with an increase in  $R_d$ , being followed by a gradual saturation. An effect of  $R_u$  on the potential formation is also measured at  $R_d = 1.68$ . But no appreciable changes of  $\Delta\phi_p$  and  $-\Delta\phi_d$  are observed even when  $R_u (>1)$  is increased up to 1.68, indicating that the results are independent of  $R_u$  as far as  $R_d \geq R_u > 1$  is kept. Thus, we can obtain almost the same results as in Fig. 5(b) even with keeping  $R_d = R_u (>1)$  (mirrors are symmetric with respect to  $z = 0$  cm).

The increase in  $P_\mu$  and/or  $R_d$  enhances the  $T_e$  anisotropy and electron trapping around the ECR point, and thus  $-\Delta\phi_d$  increases, being accompanied by an increase in  $\Delta\phi_p$  under the charge neutrality condition. Furthermore,  $\Delta\phi_p$  always saturates gradually around  $E_{i0}/e$ , plugging most of the ions so as not to pass through the magnetic well region. This is because the electrons

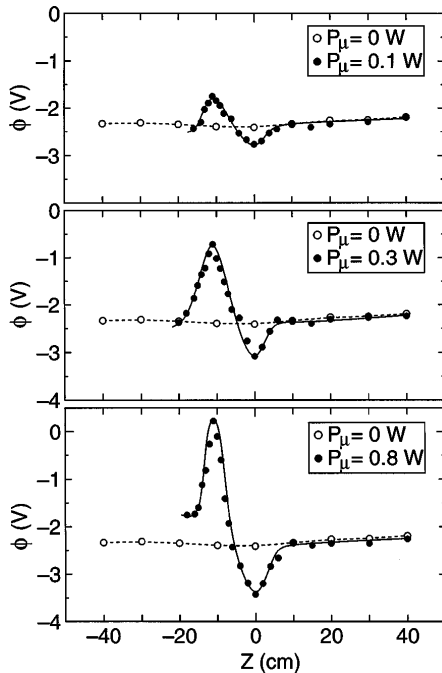


FIG. 4. Spatial profiles of  $\phi$  at  $t = 0.6$  ms with  $P_\mu$  as a parameter in the case of  $R_d = 1.68$  and  $R_u = 1.30$ .

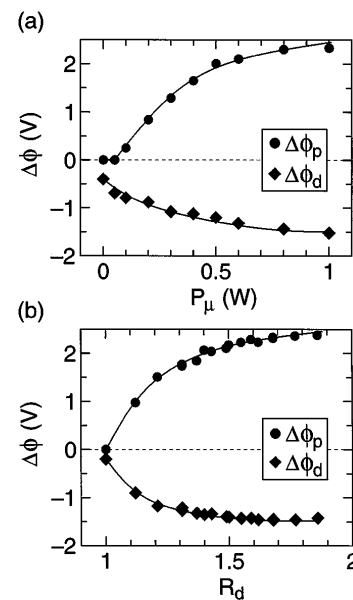


FIG. 5. Potential dip  $\Delta\phi_d$  and hump  $\Delta\phi_p$  at  $t = 0.6$  ms (a) as a function of  $P_\mu$  for  $R_d = 1.68$  and  $R_u = 1.30$  and (b) as a function of  $R_d (\geq R_u > 1)$  for  $P_\mu = 0.8$  W.

are well trapped and  $-\Delta\phi_d$  is large enough for most of the electrons to be reflected.

As described above, the potential structure observed consists of a potential dip around the ECR point and a subsequent potential hump along the plasma flow. This structure is almost the same as that in the tandem-mirror scenario with the dual ECR performance in the end mirror cells. In our experiment, the electrons accelerated by the ECR in the direction perpendicular to the magnetic field are decelerated and reflected by  $-\mu\nabla B$  in the axial direction. The electrons reflected, which are again accelerated at the ECR point, cannot return to the upstream region, being trapped in the magnetic well. This mirror trapping of electrons induces the potential dip around the ECR point. The depth is large enough to prevent cold electrons, which are supplied from the hot plate, from merging with hot electrons in the ECR region. Thus, the potential dip formed works as a "thermal-barrier" potential. Ions are not directly affected by the ECR. But, in order to satisfy the charge neutrality condition, a potential hump, a so-called "plug" potential, the height of which is large enough to reflect most of the ions flowing along the magnetic field lines, is formed in the downstream side. As a result, there appears a density decrease in the downstream region, i.e., the potential structure produced provides a "dike" potential against the plasma flow.

Our physics of the barrier/plug potential formation can also be applied to plasmas with the ion flow energy much smaller than the ion temperature. In this case, however, the flow energy  $E_{i0}$  has to be replaced by the ion temperature  $T_i$  parallel to the magnetic field. It is to be remarked that  $\Delta\phi_p/E_{i0}$  observed in our work is of the same order of  $\Delta\phi_p/T_i$  in the GAMMA 10 experiment, although  $\Delta\phi_p$  and  $E_{i0}$  in the  $Q$  machine are much smaller than  $\Delta\phi_p$  and  $T_i$  in such a big fusion-oriented device as the GAMMA 10.

In conclusion, in a collisionless plasma flow under a simple magnetic mirror configuration, a potential structure with a potential dip followed by a subsequent potential hump is formed by the ECR at the bottom of the magnetic well. Our experiment clearly demonstrates a formation of the plug potential with thermal barrier under a quite simple axisymmetric mirror configuration. The mechanism of the potential formation is based on the electron heating and trapping due to the ECR in the magnetic well under the

charge neutrality condition. It is not necessary in our potential formation to take into account the conventional scenario for the tandem-mirror devices, which needs two ECR points: the one for barrier formation and the other for plug formation. In our experiment, a single ECR point is sufficient to provide the plug/barrier potential structure. This work gives a clear physics to the formation of field-aligned plug potential with thermal barrier in a quite simplified way.

We thank Professor M. Inutake for his useful discussions and comments. Discussions with many scientists in the GAMMA 10 group were also fruitful. The authors are indebted to Y. Miyahara and H. Ishida for their assistance. The work was supported by a Grant-in-Aid for Scientific Research from the Ministry of Education, Science, Sports, and Culture, Japan.

- 
- [1] H. Alfvén and C.-G. Fälthammar, *Cosmical Electrodynamics* (Oxford University Press, London, 1963), 2nd ed., p. 162.
  - [2] Y. Serizawa and T. Sato, *Phys. Fluids* **29**, 2753 (1986); S. Ishiguro *et al.*, *Phys. Plasmas* **2**, 3271 (1995).
  - [3] N. Sato *et al.*, *Phys. Rev. Lett.* **61**, 1615 (1988).
  - [4] A. Alfvén and P. Carlqvist, *Solar Phys.* **1**, 220 (1967).
  - [5] A. Bahnsen *et al.*, *J. Geophys. Res.* **94**, 6643 (1989); M. Malingre *et al.*, *Geophys. Res. Lett.* **91**, 1339 (1992).
  - [6] D. E. Baldwin and B. G. Logan, *Phys. Rev. Lett.* **43**, 1318 (1979).
  - [7] T. Ohkawa *et al.*, *Phys. Rev. Lett.* **51**, 2101 (1983); T. Ohkawa, *Kakuyugo Kenkyu (Japan)* **64**, 305 (1990).
  - [8] D. P. Grubb *et al.*, *Phys. Rev. Lett.* **53**, 783 (1984).
  - [9] M. Inutake *et al.*, *Phys. Rev. Lett.* **55**, 939 (1985).
  - [10] T. Tamano, *Phys. Plasmas* **2**, 2321 (1995).
  - [11] C. P. Chang *et al.*, *Phys. Fluids* **31**, 123 (1988).
  - [12] T. Sato and H. Okuda, *Phys. Rev. Lett.* **44**, 740 (1980); C. Chan *et al.*, *Phys. Rev. Lett.* **52**, 1782 (1984).
  - [13] R. W. Motley, *Q Machines* (Academic, New York, 1975); N. Sato *et al.*, *Phys. Rev. Lett.* **34**, 931 (1975).
  - [14] T. Kaneko *et al.*, *Plasma Phys. Control. Fusion* **39**, A129 (1997).
  - [15] Y. Suzuki *et al.*, *J. Phys. Soc. Jpn.* **55**, 1568 (1986).
  - [16] T. Saito *et al.*, in *Proceedings of the International Conference on Open Plasma Confinement Systems for Fusion, Novosibirsk, 1993*, edited by A. A. Kabantsev (Budker Institute of Nuclear Physics, Novosibirsk, 1993), p. 121.